ON THE APPLICATION OF THE WEAKEST LINK MODEL IN THE LOWER SHELF AND TRANSITION

J.Heerens*, U. Zerbst*, H.M. Bauschke* and K.-H. Schwalbe*

The specimen size effects on fracture toughness have been investigated in the lower shelf regime. The trends of scatter, size and geometry effects observed at the lower shelf are opposite to the trend predicted by the weakest link model.
A safety assessment of surface cracks which was based on the maximum J-value along the crack front and on K_{IC}-values obtained from CT-specimens was found to be non-conservative regarding its fracture probability.
The results indicate that the classical weakest link model does not work in the lower shelf regime.

INTRODUCTION

In the transition regime the fracture toughness of steels shows large scatter, specimen size and specimen geometry effects. In order to benefit from small specimen test data strategies for dealing with theses effects are required. The most developed approach for treating scatter and size effects is based on the weakest link model (1,2,3). According to this approach the scatter of the toughness values has a Weibull distribution:

$$P_f = 1 - \exp\left(- (J / J_o)^2 \right) \qquad (1)$$

* GKSS-Research Centre Geesthacht, Institute of Materials Research, Max-Planck-Straße, Geesthacht, Germany

P_f is the cumulative probability of failure due to the initiation and extension of a cleavage crack, J is the applied J-integral and J_o and 2 are the scale parameter and the shape parameter of the Weibull distribution.

Beside modelling the scatter band of toughness, the weakest link model can also quantify specimen size effects. It is assumed that an increase of the crack front length increases the chance of sampling a weakest link at the crack front. This results in a higher probability of triggering cleavage. According to the model this sampling effect changes the scale parameter of the distribution as follows :

$$J_{oB2} = J_{oB1} \left(B_1 / B_2 \right)^{(1/2)} \qquad (2)$$

B indicates the crack front length. In many specimens the crack front length is identical to the specimen thickness.

Experience shows that Eq.1 and Eq.2 are not able to model all the experimentally observed trends of transiton toughness data. It is believed that this has two reasons:

a) Eq.1 was derived from the stress/strain field of stationary cracks. If cleavage is preceded by stable crack extension the tip fields may change and therefore Eq.1 will not be valid.

b) Eqs.1 and 2 do not account for changes of triaxiality which might occur during loading or because of a change of the size or the geometry of the specimen.

Because stable crack extension and large plastic deformation are usually observed in the transition regime but not in the lower shelf, it is expected that these effects become important for transiton data rather than for data in the lower shelf. Meanwhile extensions of the weakest link model have been proposed in order to cover constraint and ductile tearing effects (4,5,6). The potential of these approaches are currently being investigated.

In order to gain further experience with the weakest link approach, the fracture behaviour of compact specimens (CT-specimens) and surface crack tension specimens (SFC-specimens) were analysed. The main purpose of the study was to see whether the classical weakest link model presented by Eq.1 and 2 can quantify the trends of the scatter, size- and geometry effects of the toughness data obtained in the lower shelf regime.

EXPERIMENTAL DETAILS

The material used for the study was the quenched and tempered pressure vessel steel 20MnMoNi55 taken from a forged boiler bottom segment. The tensile properties at room temperature of the material are the folloing ones: Yield strength = 450 N/mm^2; Ultimate tensile strength = 610 N/mm^2; Young`s modules 210000 N/mm^2 and Reduction in area = 66%. The crack orientation was identical in all specimens including the surface crack specimens.

In order to produce a surface crack, 20 mm thick and 100 mm wide panels were pre-cracked under bending conditions. In Figure 1 the geometry of the pre-crack and the cross section of a panel is shown. The maximum crack depth, a, and the crack length, c, of the pre-crack were 10 mm and 25 mm respectively for all specimen tested. Pre-cracking of the specimens was conducted using a R-ratio of 0.1 and a Kmax-value of 450 to 600 $N/mm^{3/2}$. Side grooving (2x10%B) of the CT-specimens was done after pre-cracking using a Charpy cutter.

The fracture tests were conducted using a displacement rate of 0.5 mm/min. The test temperatures were realized using a chamber cooled by liquid nitrogen and nitrogen vapour. The specimen temperature was controlled by a thermocouple mounted near the fatigue crack tip.

For the CT-specimens the critical J-value at unstable fracture, J_c, was calculated according to ESIS P1-92. The J_c -values of the surface crack tensile panels were calculated from K_{eff} present at the deepest point of the surface crack:

$$J_{c(deep\ point)} = K_{ceff}^2/E` \qquad (3)$$

K_{ceff} was calculated from the Raju, Newman. K-solutions (7) by adding the radius of the plastic zone size to the maximum crack depth ,a, and the crack length,c. The radii of plastic zone sizes were calculated as follows:

At the deep point

$$r_a = K_c^2/(\sigma_Y^2 6\pi) \quad \text{(plane strain)} \qquad (4)$$

at the surface

$$r_c = K_c^2/(\sigma_Y^2 2\pi) \quad \text{(plane stress)} \qquad (5)$$

σ_Y indicates the yield strength which was 670 N/mm^2 at the test temperature of -150 ^oC.

RESULTS AND DISCUSSION

In Figure 2 toughness data obtained at -60 ^oC from side grooved proportional CT-specimens are presented. It can be seen that increasing the specimen size reduces the toughness. In Figure 3 these toughness data have been used to estimate the cumulative failure probability P_f of each data set by ranking the toughness values and calculating P_f as follows:

$$P_f(k) = (k-0.3)/(N + 0.4) \qquad (6)$$

N is the total number of J_c-values of a data set and k indicates the order of ranking.

In order to check the weakest link size effect prediction the scale parameter of the 20 mm thick specimens was determined by fitting the toughness data using a straight line, (this fit can be seen in Figure 8). Subsequently Eq.2 was applied to predict the scale parameters of the 50 mm and 100 mm thick specimens and Eq.1 was used to calculate P_f of the data sets. Comparing the lines and the data points in Figure 3 it can be seen that the weakest link approach (Eq.1 and 2) models the scatter and the size effects quite well.

Many of the specimens failed after substantial amounts of stable crack extension and after large plastic deformation. The initiation value for stable crack extension at this temperature is about 250 N/mm. Despite large plastic deformation and stable crack extension Eq.1 and Eq.2 seem to be sufficient to model the size effects. Corrections for constraint and stable crack extension are not required.

In Figure 4 the results from the toughness tests on CT-specimens in the lower shelf are shown. A better picture of possible size effect can be seen when the data are treated statistically by ranking the data and calculating the $P_f(k)$ -values for each data set, see Figure 5. The Figure shows that the 50 mm thick specimens have a lower failure probability than the 20 mm thick specimens. The data sets have a relatively low number of data points which may result in low statistical confidence of this conclusion.

In order to get a more confident result, an additional data set taken from Ref.(8) has been analysed in a similar way. In Figure 6 the toughness data from a pressure vessel steel A533B obtained from several proportional specimens are shown. The number of data points is quite high in this case. Arranging these data in a statistical plot, the same size effect tendency as observed for the 20MnMoNi55 specimens appears in Figure 7: Increasing the specimen size reduces the failure probability.

The toughness results obtained from the large proportional specimens, that are the CT-specimens with B=20mm, W=50mm; B=50mm,

W=100mm; 1T and 2T are valid K_{IC} data. Therefore, these results indicate that K_{IC} is a specimen size dependent quantity.

These trends of the size effects observed in the lower shelf appear to be opposite of what the weakest link approach predicts according to Eq.2. Therefore the classical weakest link approach which worked very well for the data obtained at -60 ^{o}C does not work in the lower shelf regime.

This conclusion is further supported by the Weibull plots of the toughness data in Figure 8 and Figure 9: the data sets obtained in the transition regime have a shape parameter of 2 which is in agreement Eq.1 but for the lower shelf data the shape parameter is much larger. In Figure 9 it appears that the Weibull plots have two branches rather than one single straight line as it should be according to Eq.1.

Also the morphology of the fracture surface changes significantly with the test temperature, see Fig 10a and b. In the transition regime the fracture surface shows single dominant cleavage initiation spots which refers to a weakest link type fracture, whereas in the lower shelf regime the fracture surface is basically flat and has some roughness which seems to increases with toughness. Single dominant initiation sites were not observed at the fracture surfaces in the lower shelf regime.

In Figure 11 the J_C-values of the SFC-specimens are shown. According to Ref 7 the maximum J-value along the crack is at the deepest point of the surface crack. Close to the surface the J-value reduces to about 60% of the maximum J-value for this type of surface crack. In order to compare the fracture behaviour of the CT-specimens and the SFC-specimens, the J-value at the deepest point of the surface crack was considered. In Figure 5 it can be seen that following this approach the SFC-specimens have a higher fracture probability than the CT-specimens.

It may be noted that the approach used above follows the route proposed in many assessment procedures. The results indicate that the

route of assessing the safety of surface cracks on the basis of K_{IC} obtained from CT-specimens can give non-conservative results.

CONCLUSIONS

In the lower shelf regime toughness values obtained from CT-specimens seem to be specimen size dependent. The pattern of the specimen thickness effect seem to be opposite the tendencies predicted by the weakest link model.

The trend of size effects, the morphology of the fracture surfaces and the behaviour of the Weibull plots promote the assumption that other approaches than the classical weakest link model are required to model size effects and scatter in the lower shelf.

In the lower shelf the safety assessment of surface cracks which was based on the maximum J-value along the crack front and on K_{IC}-values obtained from CT-specimens was found to be non-conservative

Acknowledgements: Thanks are due to Dipl.-Ing. Jürgen Knaack for running some of the surface crack tests. Thanks also to Olaf Kreienbring for technical assistance.

REFERENCES

(1) J.D. Landes and G.H Shaffer, Fracture Mechanics: Twelfth Conference, ASTM STP 700, 1980, pp.368-378

(2) K. Wallin, T. Saario and K. Törrönen, Metal. Sci., Vol. 18,1984,pp.13-16

(3) S. Slatcher, Fatigue Fract. Engng. Material, Struct, 1986

(4) W. Ehl, Bruchmechanische, statistische und fractographische Untersuchungen am Stahl 20MnMoNi55 im Übergangsbereich, Dissertation TU-Karlsruhe, 1987

(5) K. Wallin, Eng. Frac. Mech, Vol. 32, 1989, pp.523-531

(6) T.L. Anderson and R.H. Dodds, Journal of Testing and Evaluation, Vol 19, 1991, pp. 123-134

(7) I.S. Raju and J.C Newman, Eng. and Fract. Mech. Vol. 11,1979, pp. 817-829

(8) D.E. McCabe, Okridge National Laboratories, private communication

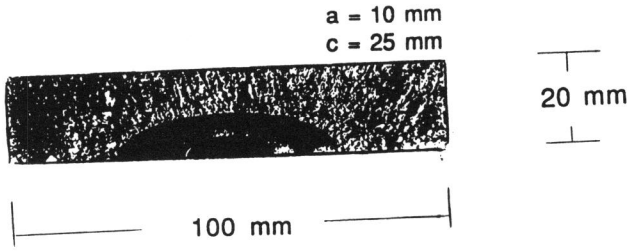

Fig.1 Geometry of the surface crack and cross-section of the SFC-panels (20MnMoNi55).

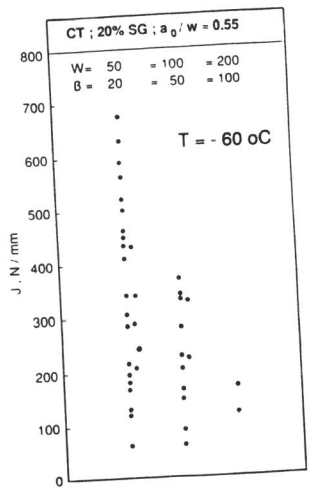

Fig.2 Effect of CT-specimen size on fracture toughness of 20MnMoNi55 obtained in the transition regime.

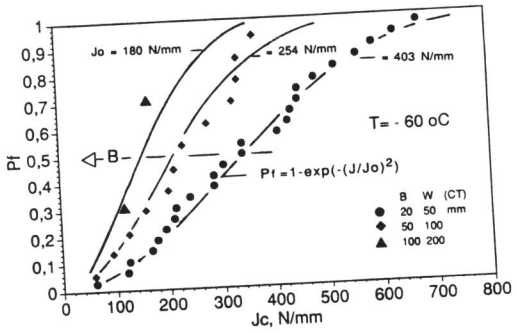

Fig.3 Prediction of the cumulative failure probability of the data of Fig.2 using the weakest link model (lines indicate the prediction).

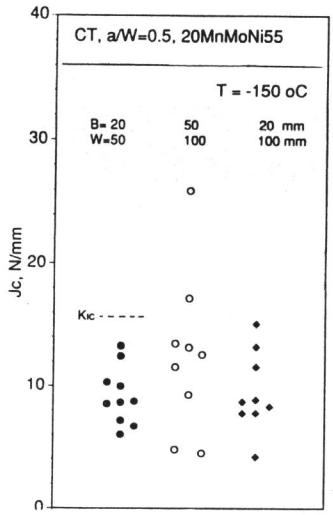

Fig.4 Scatter of the fracture toughness of 20MnMoNi55 at the lower shelf determined using different CT-specimens.

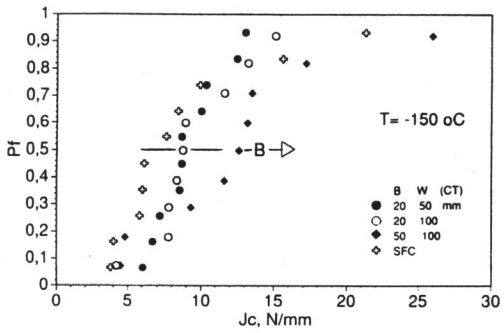

Fig.5 Influence of specimens size of the cumulative failure probability of the 20MnMoNi55 toughness data shown in Fig. 4.

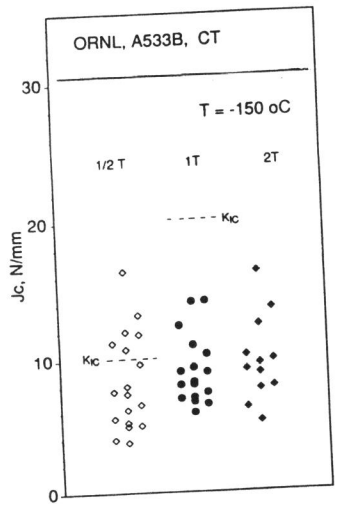

Fig.6 Scatter of the fracture toughness of A533B at the lower shelf determined using different CT-specimens (data taken from Ref. 8).

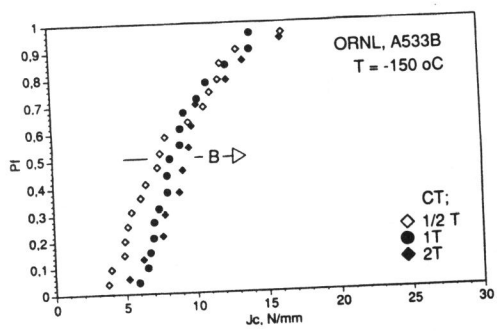

Fig.7 Influence of specimens size of the cumulative failure probability of the A533B toughness data shown in Fig. 6.

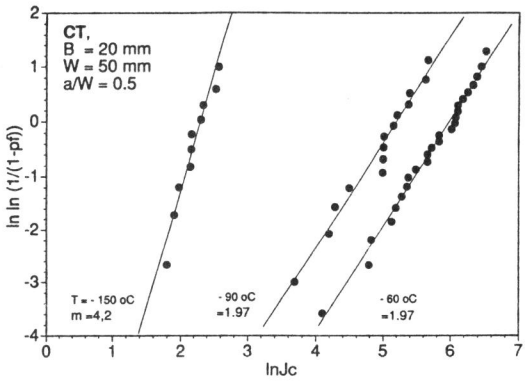

Fig.8 Influence of temperature on the Weibull-plots (Material:20MnMoNi55).

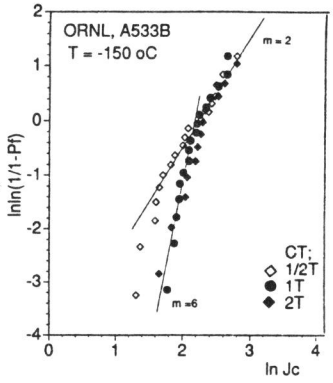

Fig.9 Weibull-plots of the lower shelf data of A533B.

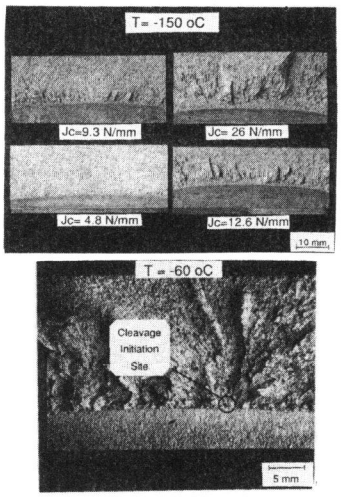

Fig.10 Comparison of the fracture surface morphology obtained in the transition regime and in the lower shelf.

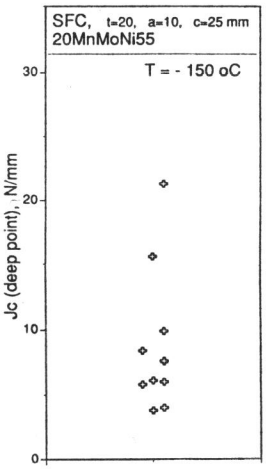

Fig.11 J-values at the deepest point of the surface cracks at the moment of unstable fracture.